

Original Article

miR-127-5p regulates FAIM2-mediated cell apoptosis and participates in cerebral ischemia-reperfusion injury

Teng Hu^{1,2}, Yongzhong Lin^{1*}

¹ Department of Neurology, The Second Affiliated Hospital of Dalian Medical University, Dalian, Liaoning Province, 116021, China

² Department of Neurointervention and Neurointensive Care, Central Hospital of Dalian University of Technology, Dalian, Liaoning Province, 116033, China

Article Info

Abstract



Article history:

Received: September 09, 2023

Accepted: December 09, 2023

Published: February 29, 2024

Use your device to scan and read the article online



Mechanical thrombectomy (MT) has become an effective re-airway method for cerebral ischemia-reperfusion injury (CI/RI). However, at present, there are few studies on the impact of MT therapy on the prognosis of CI/RI patients at home and abroad. Therefore, this paper aims to analyze the relevant factors affecting the prognosis of CI/RI patients after MT therapy. The main regulatory miRNAs during CI/RI in patients with MT were screened and studied. Serums were obtained from 80 patients (moderate to severe stroke) who underwent MT. Clinical information was recorded using a unified standard questionnaire. According to the modified Rankin Scale, the patients were divided into a good prognosis group and a poor prognosis group. The clinical data were compared respectively, and univariate and multivariate Logistic regression analysis was performed. ROC curves were drawn, and Kaplan-Merier method determined whether different NIHSS scores at admission had any difference in the in-hospital survival rate of CI/RI patients treated with MT. miRNAs in serum were detected and screened out. Cell and animal models were established, in which miRNAs and apoptotic molecules were detected. miRNA target genes were predicted, and the mechanism of miRNA regulation of apoptosis was verified. Gender, smoking, drinking, diabetes, hypertension, hyperlipidemia, age, and alcohol consumption suggested no difference in the two groups. The rates of smoking history, diabetes, hypertension, and hyperlipidemia in the poor prognosis group were higher than those in the good prognosis group. Smoking and diabetes were independent risk factors for poor prognosis. miR-127-5p expression in CI/RI patients with poor prognosis was higher than that in those with good prognosis. miR-127-5p expression was also elevated in both cell and animal models. Cell apoptosis was weakened after miR-127-5p knockdown, and tissue infarction in animal models was also reduced. FAIM2 was a target gene of miR-127-5p. silencing FAIM2 enhanced apoptosis after miR-127-5p knockdown. miR-127-5p/FAIM2 axis can be a new strategy to treat and prevent brain injury in CI/RI patients treated with MT.

Keywords: Apoptosis, Cerebral stroke, FAIM2, Mechanical thrombectomy, miR-127-5p, Reperfusion

1. Introduction

Ischemia is defined as a lack of blood supply to tissues due to blocked arterial flow [1]. When blood supply is re-established after ischemia, local inflammation and ROS production increase, giving rise to the concept of "ischemia/reperfusion (I/R) injury" [2]. A range of drugs and interventional therapies have emerged to reduce oxidative stress, inflammation, and apoptosis in the brain [3]. Recombinant tissue plasminogen activator (rt-PA) is currently the only drug approved for restoring blood perfusion, but reperfusion injury and narrow window treatment time limit its use in most stroke patients [4]. Mechanical thrombectomy is an effective treatment for ischemic stroke, and the combination of stent thrombectomy and intravenous thrombolysis has a significant effect on distal carotid artery occlusion or proximal middle cerebral artery occlusion within 6 h of symptom onset of acute ischemic stroke [5].

However, patients are at a high risk of developing common complications after undergoing MT [6]. Therefore, the study of the mechanism of reperfusion injury after MT provides a new therapeutic target for patients with MT.

After ischemic hypoxic stress, cellular and molecular events trigger dysregulation of different miRNAs, which are responsible for the long-term progression and expansion of neuronal damage. Due to their ability to modulate target protein synthesis [7], miRNAs emerge as a possible therapeutic strategy to limit neuronal damage following cerebral ischemic events [8]. For instance, miR-23a-3p [9], miR-181b [10], miR-128, and miR-496 [11] have been implicated dysregulated in cerebral ischemic events, and all of them have therapeutic potential to alleviate pathological injuries in the disease condition. miR-127 has been studied as a mechanistic element involved in I/R injuries [12, 13]. Moreover, it has been proposed that hsa-miR-

* Corresponding author.

E-mail address: lin19671024@hotmail.com (Y. Lin).

Doi: <http://dx.doi.org/10.14715/cmb/2024.70.2.27>

127-5p is a potential diagnostic biomarker for myocardial infarction [14]. However, whether miR-127-5p mediates CI/RI progression by controlling cell apoptosis is incompletely defined.

Therefore, our research studied miR-127-5p and its target FAIM2 in the process of CI/RI in the scenario of patients with acute ischemia stroke developing MT reperfusion injury. Based on the study, it is hoped to explain the miRNA-based mechanism and molecule-based therapies for CI/RI.

2. Materials and methods

2.1. Clinical Data

80 patients with moderate to severe stroke who were hospitalized in Dalian Municipal Central Hospital from October 2021 to October 2022 and underwent thrombectomy for acute large vessel occlusion were selected. Age, gender, blood pressure, fasting blood glucose, blood lipids, baseline ASPECT score, and other clinical and laboratory indicators were collected for all enrolled patients. Successful thrombolysis after surgery was evaluated using modified thrombolysis in cerebral infarction (mTICI) scale, which was defined as grade 2b and grade 3. All patients were recorded on the modified Rankin score scale (mRS Score) 7 days after the onset of the disease. The patients were divided into 2 groups, including a good prognosis group (≤ 2 mRS scores) and a poor prognosis group (> 2 mRS scores).

2.1.1. Inclusion criteria

(1) mRS Scores before stroke ranged from 0 to 1; (2) Ischemic stroke caused by large blood vessel occlusion (such as an internal carotid artery, middle cerebral artery M1 segment); (3) Age ≥ 18 years old; (4) NIHSS score ≥ 6 points; (5) Scores in ASPECTS ≥ 6 ; (6) Treatment can be started within 6 h of onset (femoral artery puncture); (7) TICI $\geq 2b$.

2.1.2. Exclusion criteria

(1) Intracranial hemorrhage confirmed by head CT or MRI; (2) Pre-onset mRS Score ≥ 2 points; (3) Pregnant or lactating women; (4) Contrast agent or Nitinol allergy; (5) Participating in other clinical trials; (6) Systolic blood pressure > 185 mmHg or diastolic blood pressure > 110 mmHg that cannot be controlled by antihypertensive drugs; (7) Genetics or acquired bleeding constitution, lack of anticoagulation factors; Or have taken oral anticoagulants with INR > 1.7 ; (8) Blood glucose < 50 mg/dl (2.8 mmol/L), or > 400 mg/dl (22.2 mmol/L), platelets $< 50 \times 10^9/L$, or hematocrit $< 25\%$; (9) The artery is severely tortuous artery and the thrombectomy device is expected to fail to reach the target vessel; (10) Postoperative life expectancy < 7 days; (11) Acute ischemic cerebral infarction occurred within 48 h after percutaneous coronary or cerebrovascular interventional surgery or major surgery; (12) A history of cerebrovascular inflammation with clear evidence; (13) Neurological diseases or mental disorders before onset, which affected the condition assessment. The study was approved by the Ethics Committee of Dalian Municipal Central Hospital, and all enrolled subjects signed informed consent.

2.2. Sampling

Direct arterial thrombectomy or bridging arterial

thrombectomy was used. The intravenous thrombolytic drugs were rt-PA and urokinase. The dosage of rt-PA was 0.9 mg/kg, the maximum dose was 90 mg, the first administration (10%) was performed with intravenous injection within 1 min, and the remaining administration was performed with intravenous micropump injection for 1 h. Urokinase (1-1.5 million IU) was dissolved in 100 to 200 mL isotonic sodium chloride solution and administered by intravenous infusion for 30 min. The bridging artery thrombectomy was performed while intravenous thrombolysis was performed. If it was found that the responsible artery was not recanalized during the angiography, the thrombus was removed through the blood flow reconstruction device. During the operation, stents, balloon dilation, and antiplatelet drugs were used according to clinical needs.

2.3. Cell culture

SH-SY5Y cells were cultured in a DMEM-F12 (1:1) medium containing 10% fetal bovine serum and 1% penicillin/streptomycin with 5% CO₂ at 37°C. The cell growth was observed every day, and the time of liquid change was determined according to the color change of the medium. Cell passage was performed when the cell growth reached about 80% confluence. At the time of passage, cells were washed with PBS solution 3 times, and then 2 mL of 0.25% trypsin was added for 2-min digestion. Then, 3 mL of complete medium was added to terminate digestion, and the adherent cells were prepared into a cell suspension. After centrifugation at 1000 rpm for 4 min, the supernatant was discarded and 1 mL of complete medium was added to re-suspend the cells. According to the growth state of the cells, the cells were cultured at 37°C and 5% CO₂ in a ratio of 1:2 to 1:10.

2.4. Cell transfection

The old medium was discarded when the cells reached 80% confluence, and the cells were washed with PBS 3 times, added with 1.5 ml serum-free medium, and transfected 2 h later. Then, 6 μ l Lipofectamine 3000 and 3000 ng plasmid were added into 250 μ l serum-free medium and left at room temperature for 5 min, respectively. The two mixture was combined for 20 min, and the medium was changed after 4-6 h.

2.5. OGD/R cell model

The chemical anoxia method plus glucose-free medium was utilized for OGD. T25 cell culture bottles and oxygen indicator were put into a 350 ml anaerobic bag (Mitsubishi) and sealed. The bag was placed in an incubator at 37°C, 5%CO₂, and 95% air for 4 h. The color of the oxygen indicator after hypoxia was changed from light blue to dark blue (O₂ $> 0.5\%$) to light purple to pink (O₂ $< 0.1\%$). The glucose-free medium was replaced by a complete culture based on glucose reoxygenation in a 5%CO₂ incubator at 37°C. The control group was cultured conventionally.

2.6. OGD/R animal model

This animal experiment was approved by the Ethics Committee of Dalian Municipal Central Hospital. The Middle Cerebral Artery Occlusion (MCAO) model was studied by intravenous injection of 10% chloral hydrate at 0.3 mL/100 g body weight. After the anesthesia took

effect, the rats were fixed with tape, and the median incision of the neck was made. After odor sterilization, the right common carotid artery (CCA), internal carotid artery (ICA), and external carotid artery (ECA) were isolated, and the ECA and CCA were ligated. A silk thread was reserved near the CCA bifurcation, the ICA was clipped with an artery clamp at the proximal end, and a small incision was made at the CCA about 1 cm from the bifurcation with ophthalmic curved scissors. The tying suture was marked at 23 mm, 20 mm, and 18 mm in length, and the tying suture was inserted into the ICA from the incision. When reaching the artery clamp, a slip-knot was tied on the CCA reserve thread, the artery clamp was released, and the tying suture was inserted into the ICA. When the tying suture was felt to have significant resistance, the tip of the tying suture was inserted into the right middle cerebral artery. At this time, the reserved thread was tied tightly and the exposed thread was cut, then the skin was sewed and sterilized with alcohol. After 2 h of embolization, the tying suture was removed and reperfusion was performed for 24 h. In the sham operation group, no MCAO was performed. SD rats were placed in a clean rat cage alone after modeling and scored after anesthesia. Head CT scan was performed 24 h after the operation, and low-density areas of brain tissue in the right middle cerebral artery blood supply area indicated that the local blood supply was impaired, indicating that the modeling was successful.

2.7. CCK-8 detection

The proliferation of SH-SY5Y cells at 0, 24, 48, and 72 h after transfection was assessed using CCK-8 kits (Dojindo, Japan). Cells were placed in 96-well plates at 2×10^3 cells/well and incubated routinely. At 0, 24, 48, and 72 h, 10 μ L of CCK-8 reagent was added and incubated for 2 h before recording the absorbance at 450 nm on a microplate reader (Bio-Rad, USA).

2.8. Flow cytometry

Cells were resuspended in pre-cooled PBS, centrifuged at 4°C for 5 min, and washed with PBS twice for 5 min. Then, 200 μ L binding buffer was added, followed by 5 μ L Annexin V-FITC for 15 min and 10 μ L PI solution for 10 min. Annexin V-FITC (green) fluorescence intensity and PI (red) fluorescence intensity were detected by flow cytometry after filtration with 400 μ L binding buffer.

2.9. Dual-luciferase reporter gene assay

TargetScan (http://www.targetscan.org/vert_71/) and

starBase 7.1 3.0 predicted miR-127-5p' targets. FAIM2 3'UTR sequence containing the miR-127-5p binding site was inserted into the pmirGLO vector. The cells reaching the logarithmic phase of growth were co-transfected with the reporter and miR-127-5p mimics or control mimics using Lipofectamine® 2000. After 48 h, cells were lysed with a lysis buffer (100 μ L/well) using dual luciferase reporter assay kits (Beyotime, China) and centrifuged at 10,000-15,000 g for 3-5 min. The supernatant was taken to detect luciferase activities.

2.10. Protein immunoblotting

Peripheral venous blood of 3 mL was extracted from the patients before surgery, 24 h and 72 h after surgery, and placed in an anticoagulation tube. Serum was collected after centrifugation at 3000 r/min at 4°C for 10 min. The collected serum was transferred to a separate frozen storage tube for short-term storage and put in a -70°C refrigerator, and stored in liquid nitrogen for long-term storage. Sufficient dry ice must be used during transportation to keep temperatures low. The amount of dry ice should be at least 8 kg, the thick wall foam box should be used for transportation, and the box should be sealed with sealing tape. In the process of sample preservation and transfer, repeated freezing and thawing should be avoided. Total RNA was extracted from the samples using RNeasy Mini Kit and quantitatively determined by Nano Drop2000 microspectrophotometer. The qualified RNA specimens were placed at -80 °C for use. If the D260/D280 of the RNA sample is < 2.0, the RNA is extracted again.

2.11. RT-qPCR

MolPure® Cell/Tissue Total RNA Kit (YEASEN, Shanghai, China) was employed to extract total RNA from tissue or cultured cells. RNA from the nucleus and cytoplasm was isolated using the PARIS kit (Life Technologies, USA). RNA concentration and purity were assessed using a NanoDrop 2000 spectrophotometer (Thermo Fisher Scientific). PCR was performed on the LightCycler 480 real-time PCR instrument (Roche, Switzerland) using Hieff®qPCR SYBR®Green Master Mix Kit (YEASEN). RNA expression was calculated by $2^{-\Delta\Delta Ct}$ method and standardized to GAPDH. All primers for RT-qPCR are listed in Table 1.

2.12. TUNEL staining

The cells were incubated with protease K, the sections were immersed in TUNEL solution and then washed with

Table 1. Primer sequences.

Name	sequence	Tm	pb
miR-127	F: GGAAGATCTGTAGTCCTGTCTGTTGGTCAG	57	160
	R: CCAAGCTTCCTGAAGAACTGCTCCGCC	53.6	
miR-23a	F: GCCGCGGGGTTCCCTGGGGAT	55.2	157
	R: GTGCAGGGTCCGAGGT	54.5	
miR-181b	F: CTCAACTGGTGTCTGAGTCGGCAATTCAGTTGAGAACCCACC	50	157
	R: ACACTCCAGCTGGGAACATTCATTGCTGTCTCGG	52.9	
miR-128	F: TGCGGTCACAGTGAACCGGTCTC	54.3	145
	R: CCAGTGCAGGGTCCGAGGT	51.2	
miR-496	F: CCAAGUCAGGUACUCGAAUGGAGGUUGUCCAUGGUGUGUUCAUUUU	54.2	146
	R: AUUUUAUGAUGAGUAUUACAUGGCCAAUCUCCUUUCGGUACUCAAUUCUUCUUGGG	53.6	
U6	F: CTCGCTTCGGCAGCACA	60.1	155
	R: AACGCTTCACGAATTTGCGT	62	

PBS 3 times. After rinsing with hydrogen peroxide, the enzyme activity was quenched and coated with anti-biological protein catalase and DAB. The apoptotic nuclei (observed in 5 fields) were brown and yellow under a high-power optical microscope. Apoptosis rate: number of apoptotic cells/total number of cells \times 100%.

2.13. Statistical analysis

Data assessment was conducted using SPSS 19.0 software. The normally distributed measurement data were presented as $\bar{x} \pm s$. Enumeration data were compared using the χ^2 test. Binary logistic regression analysis was performed to compare the influence of each factor on the prognosis of patients, with $\alpha = 0.05$. Analytical data were labeled as mean \pm standard deviation ($\bar{x} \pm s$) and plotted using Graph Prism 5.0.

3. Results

3.1. General information

No significant changes were seen in gender, smoking, drinking, diabetes, hypertension, and hyperlipidemia between the two groups ($P > 0.05$, Table 2).

3.2. Analysis of patient prognosis

82 CI/RI patients were divided into a poor prognosis group (30 patients with ≥ 2 scores) and a good prognosis

group (52 patients with < 2 scores) according to mRs. No significant difference was observed in age or alcohol consumption between the two groups ($P > 0.05$). Compared with the good prognosis group, the rates of smoking history, diabetes, hypertension, and hyperlipidemia in the poor prognosis group were increased ($P < 0.05$, Table 3).

3.3. Binary logistic regression analysis of poor prognosis

With the patient's prognosis as the dependent variable, and age, gender, smoking, drinking, diabetes, hypertension, and hyperlipidemia as the independent variables, smoking and diabetes were independent risk factors for poor prognosis through the analysis of binary Logistic regression equation (Table 4).

3.4. Changes in serum miRNAs expression

RT-qPCR results showed no statistical significance in miR-23a, miR-181b, miR-128, and miR-496 in the carotid artery, jugular vein, and femoral vein ($P > 0.05$, Figures 1A, C-E). In addition, miR-127-5p showed no significant difference in the carotid artery and jugular vein between the two groups ($P > 0.05$). miR-127-5p was significantly different in the femoral vein between the two groups ($P < 0.05$, Figure 1B).

Table 2. Comparison of general data between the two groups.

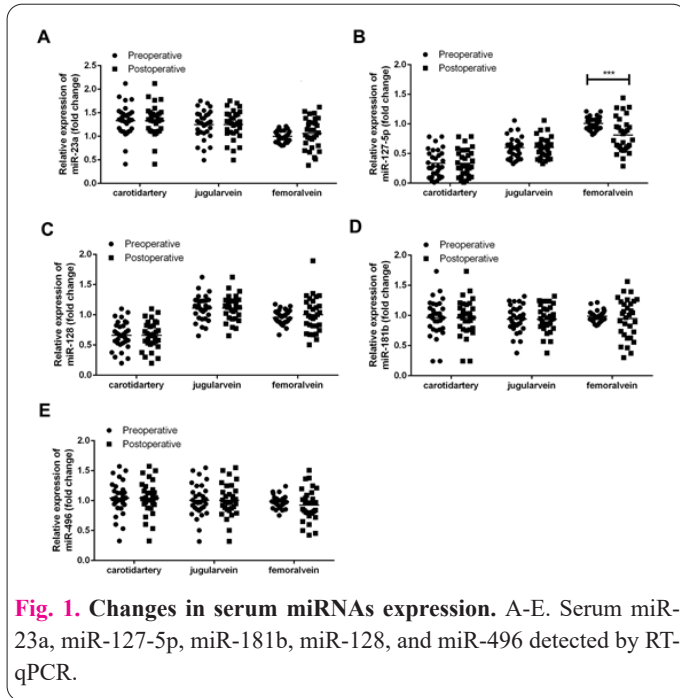
		Normal group (n = 80)	Patient group (n = 82)	t/χ^2	P
Age (years)		61.16 \pm 10.51	58.26 \pm 8.98	0.913	0.367
Gender	Male	45	39	1.225	0.268
	Female	35	43		
Smoking	Yes	44	42	0.232	0.63
	No	36	40		
Drinking	Yes	55	60	0.384	0.535
	No	25	22		
Diabetes	Yes	33	35	0.034	0.853
	No	47	47		
Hypertension	Yes	33	46	3.573	0.059
	No	47	36		
Hyperlipidemia	Yes	16	23	1.435	0.231
	No	64	59		

Table 3. Comparison of general data between the two groups.

		Poor prognosis (n = 30)	Good prognosis (n = 52)	t/χ^2	P
Age (years)		59.41 \pm 7.36	59.32 \pm 8.64	0.047	0.963
Gender	Male	14	25	0.015	0.902
	Female	16	27		
Smoking	Yes	27	15	28.476	0
	No	3	37		
Drinking	Yes	22	38	0.001	0.98
	No	8	14		
Diabetes	Yes	22	13	18.166	0
	No	8	39		
Hypertension	Yes	26	20	17.95	0
	No	4	32		
Hyperlipidemia	Yes	15	8	11.295	0.001
	No	15	44		

Table 4. Results of binary Logistic regression analysis of poor prognosis.

Variables	β	SE	Wald χ^2	P	OR	95%CI
Age	0.052	0.049	1.117	0.291	1.053	0.957-1.159
Gender	-1.227	0.844	2.117	0.146	0.293	0.056-1.531
Smoking	2.547	0.945	7.264	0.007	12.773	2.003-81.436
Drinking	-1.019	0.775	1.729	0.189	0.361	0.079-1.649
Diabetes	2.044	0.783	6.815	0.009	7.725	1.665-35.851
Hypertension	1.063	1.016	1.094	0.295	2.894	0.395-21.188
Hyperlipemia	1.482	0.899	2.715	0.099	4.402	0.755-25.653



3.5. Diagnostic value of miRNAs in CI/RI

According to ROC analysis, serum miRNAs within 8 h after the onset of the disease were measured. The ACU of miR-128 was 0.839 (0.770-0.907), the sensitivity was 88.30%, and the specificity was 63.30%. The ACU of miR-23a was 0.787 (0.706-0.867), the sensitivity was 78.30%, and the specificity was 71.70%. The ACU of miR-127 was 0.772 (0.687-0.858), the sensitivity was 80.00%, and the specificity was 76.83%. The ACU of miR-181b was 0.761 (0.681-0.844), the sensitivity was 81.22%, and the specificity was 72.22%. The ACU of miR-496 was 0.754 (0.672 -- 0.831), the sensitivity was 80.19%, and the specificity was 71.98%. The results of combined detection showed that the ACU was 0.945 (0.905-0.984), the sensitivity was 86.70%, and the specificity was 91.20%, all of which were higher than each miRNA (Figure 2).

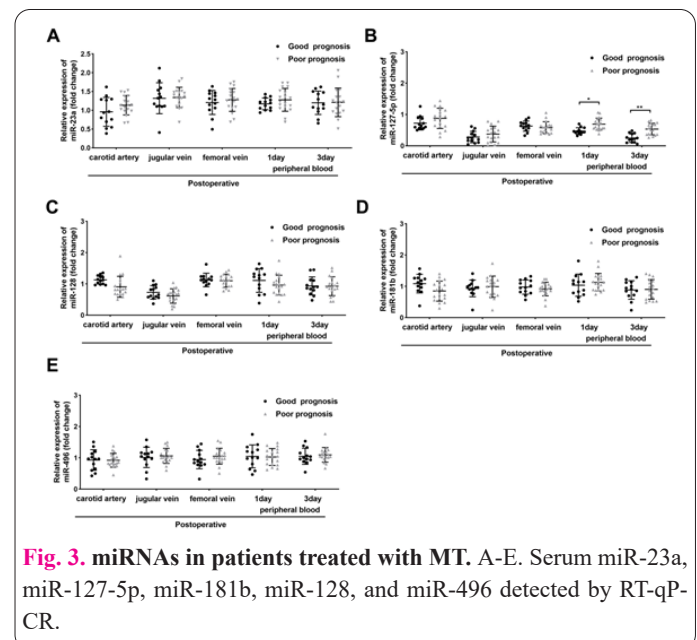
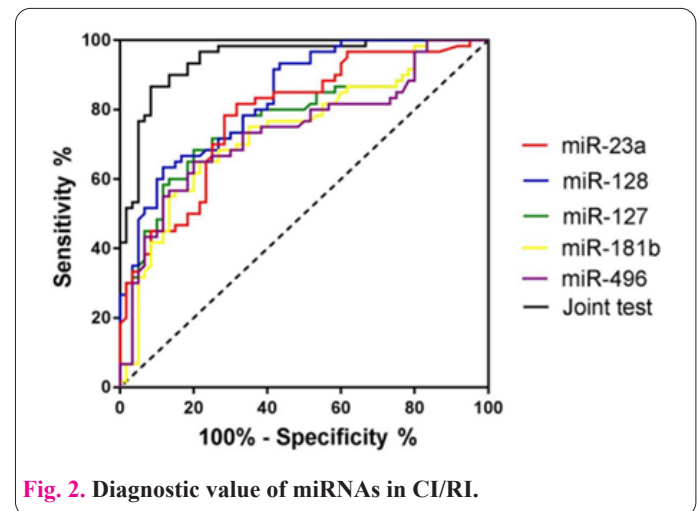
3.6. Expression of miRNA in patients treated with MT

The patients were treated with intravenous thrombolytic drugs rt-PA and urokinase, respectively, and 3 mL of peripheral venous blood was drawn. RT-qPCR results showed that comparison of miR-23a, miR-128, miR-181b, and miR-496 in the carotid artery, jugular vein, and femoral vein showed no statistical significance at 24 h and 72 h after treatment ($P>0.05$, Figures 3A, C-E). No significant difference was shown in miR-127-5p in the carotid artery, jugular vein, and femoral vein at 24 h and 72 h after treatment ($P>0.05$). The difference between miR-127-5p was statistically significant ($P<0.05$, Figure 3B), and the

difference was most obvious at 72 h after treatment. In addition, miR-23a, miR-127-5p, and miR-128 expression in pre-operative jugular vein and pre-operative femoral vein were significantly different ($P<0.05$). Compared with the normal group, pre-operative miR-23a expression was up-regulated in the jugular vein and showed no significant difference in the femoral vein, pre-operative miR-127-5p was down-regulated in the jugular vein and femoral vein, and pre-operative miR-128 was down-regulated in jugular vein and presented no significant difference in the femoral vein (Figure 3B).

3.7. miR-127-5p promotes apoptosis of neurons

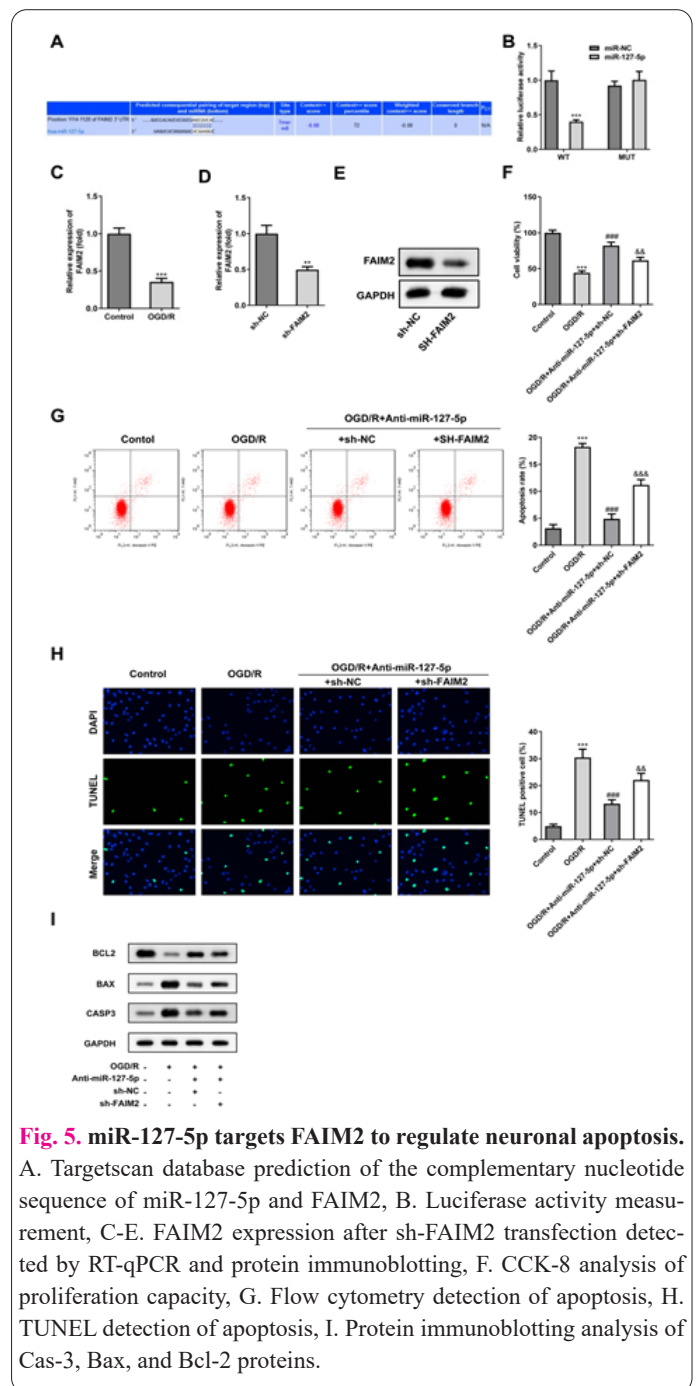
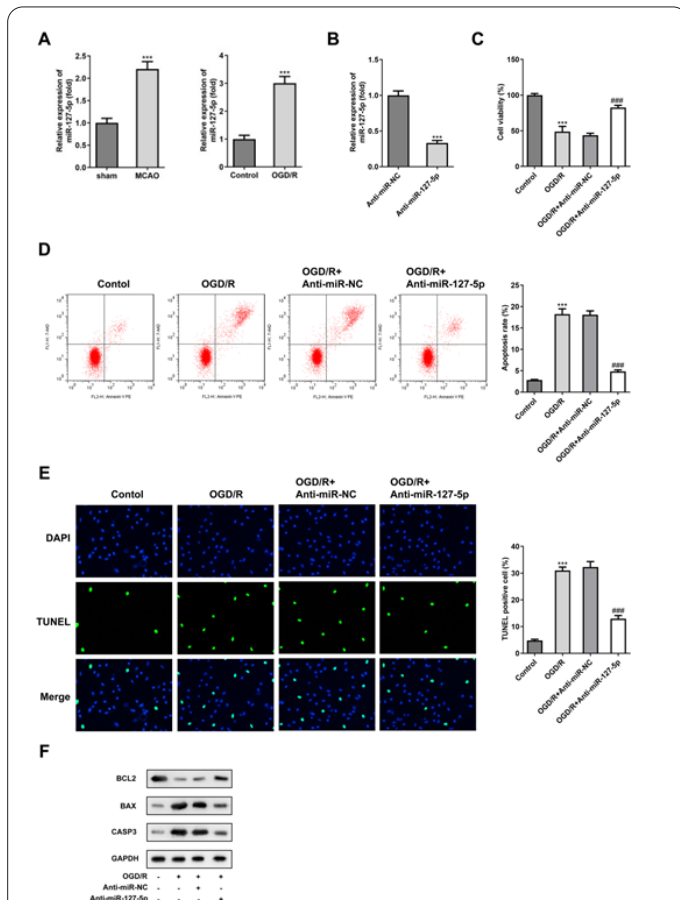
MCAO animal models and OGD/R cell models were constructed to analyze miR-127-5p's function. PCR-re-



sults manifested that miR-127-5p was up-regulated in both MCAO animal models and OGD/R cell models (Figure 4A). In OGD/R cell models, miR-127-5p expression was suppressed after transfection with anti-miR-127-5p, indicating successful transfection (Figure 4B). CCK-8 results determined that miR-127-5p inhibition significantly increased cell proliferation (Figure 4C), whilst flow cytometry analysis showed that miR-127-5p inhibition increased cell survival and decreased apoptosis rate (Figure 4D). TUNEL results showed that OGD/R treatment resulted in a significant increase in cell death. Transfection with anti-miR-NC did not affect OGD/R cell death, while transfection with anti-miR-127-5p resulted in a significant decrease in OGD/R-induced cell death (Figure 4E). Protein immunoblotting results discovered that Anti-miR-127-5p could significantly reverse OGD/R-induced apoptosis-related proteins Cas-3, Bax, and Bcl-2 (Figure 4F).

3.8. miR-127-5p targets FAIM2 to regulate neuronal apoptosis

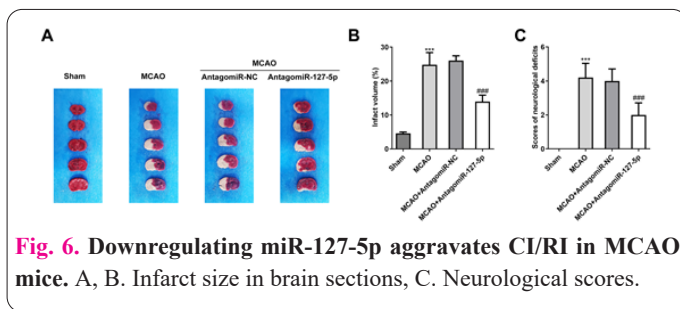
TargetScan and miRBase were utilized to predict the mRNAs that could target miR-127-5p, and verified the candidate mRNAs by RT-qPCR analysis through dual luciferase reporter vector assay (Figure 5A). Significantly decreased luciferase reporter gene activity was detected in cells co-transfected with FAIM2-WT vector, while the activity detected by FAIM2-MUT vector did not change significantly (Figure 5B). PCR results demonstrated that



FAIM2 expression was down-regulated in the OGD/R cell model. However, FAIM2 expression was up-regulated by transfecting with Anti-miR-127-5p (Figure 5C). FAIM2 expression was significantly suppressed by transfecting with sh-FAIM2, indicating successful transfection (Figures 5D, E). CCK-8 results highlighted that after transfection with sh-FAIM2, the enhanced cell viability and decreased apoptosis induced by miR-127-5p inhibition were reversed (Figures 5F-H). sh-FAIM2 was also able to reverse the effects of Anti-miR-127-5p on apoptosis-related proteins Cas-3, Bax, and Bcl-2 (Figure 5I).

3.9. Downregulating miR-127-5p aggravates CI/RI in MCAO mice

The effect of miR-127-5p knockdown on MCAO mice was studied by microinjection of antagomiR-NC or antagomiR-127-5p adenovirus into the lateral ventricle. Two weeks after injection, green fluorescent protein (GFP) adenoviruses were largely limited to the whole brain. The infarct area in the brain tissue of the MCAO mice was the



largest, while antagomiR-127-5p reduced the infarct area (Figures 6A, B), and the neural scores of the mice injected with antagomiR-127-5p were significantly higher than those of MCAO mice (Figure 6C).

4. Discussion

Smoking has been identified as a major risk factor for severe myocardial injury after reperfusion, which exceeds other known risk factors [15]. It has been illustrated that smoking has a relationship with slow recovery in peripheral nerve I/RI [16]. Diabetes mellitus is a common complication of ischemic stroke and is characterized by hyperglycemia [17, 18] and can increase organ susceptibility to ischemia-reperfusion injury and alter responses to ischemia-adaptive strategies [19]. Moreover, hypertension is a vulnerable index for I/RI [20], as well as hyperlipemia [21]. The four indices have suggested a relationship with poor prognosis in CI/RI patients in this study. Furthermore, smoking and diabetes were independent risk factors for poor prognosis.

Pharmacological approaches to inhibiting miRNAs seem likely to be the way to treat patients in the process of I/RI [22]. Consistent with this concept, this research analyzed the involvement of miRNAs in CI/RI. Analysis of serum miRNAs in CI/RI patients found no significance in miR-23a, miR-181b, miR-128, and miR-496 in those with good prognosis and poor prognosis, but not in miR-127-5p in the femoral vein, suggesting an association between serum miR-127-5p level and patient's prognosis. Clinically, the detection of serum markers provides a diagnostic value in diseases [23, 24]. In this research, combined detection of miR-23a, miR-127, miR-181b, miR-128, and miR-496 had an ACU of 0.945 (0.905-0.984), sensitivity of 86.70%, and specificity of 91.20%, which were higher than independent detection of each miRNA. These findings expand the field of serum marker detection in the diagnosis of CI/RI.

Among the 5 studied miRNAs, only miR-127-5p expression was significant after MT therapy, implying that miR-127-5p may be involved in CI/RI. To further analyze the function of miR-127-5p in CI/RI, OGD/R-treated cells were interfered with miR-127-5p inhibition, contributing to the promotion of proliferation and the suppression of apoptosis and death. miR-127-5p has been defined as a tumor suppressor [25-27] that is associated with the malignant progression of tumor growth. Additionally, studies have shown the regulatory involvement of miR-127-5p in osteoarthritis in part by controlling apoptosis and proliferation of chondrocytes [28-30]. In addition to cell experiments, animal experiments were conducted on MCAO mice to confirm the neuroprotective effects of antagomiR-127-5p, as manifested by reduced infarct area and improved nervous system function. Prior to this study, no other studies had explored the function and related mechanisms

of miR-127-5p in MT reperfusion after ischemic stroke.

FAIM2 is an anti-apoptotic protein that uniquely protects cells from FAS-induced apoptosis. FAIM2 regulates FAS-mediated neuronal apoptosis by interfering with caspase-8 activation. In this research, FAIM2 was studied as a target of miR-127-5p. FAIM2 was downregulated in OGD/R-treated cells and its expression level was mediated by miR-127-5p. In regard to the function of FAIM2, this study determined that FAIM2 silencing mitigated the action of miR-127-5p knockdown on OGD/R-treated cells, resulting in the enhancement of apoptosis and reduction of cellular apoptosis. Deficiency of FAIM2 leads to increased susceptibility of primary neurons to OGD in vitro, as well as caspase-related cell death and nerve damage after cerebral ischemia in vivo [31]. It has been reported that FAIM2 up-regulation may be involved in the neuroprotective effect of low-dose erythropoietin on transient cerebral ischemia [32]. FAIM2 loss results in increased degeneration of dopaminergic neurons, suggesting that FAS-induced apoptosis promotes cell death in Parkinson's disease [33]. It is observable that FAIM2 deficiency increases cleaved-caspase 3 and Bax levels in primary murine cortical neurons subjected to OGD, while FAIM2 upregulation can reduce cell apoptosis after OGD [34].

In short, targeted inhibition of miR-127-5p expression or increase of FAIM2 expression can reverse the apoptosis process, thereby alleviating ischemia injury in patients treated with MT. Therefore, the regulation of miR-127-5p and FAIM2 may be a new strategy to treat and prevent CI/RI. This study only evaluated the in vivo action of miR-127-5p, and that of FAIM2 was not investigated, which should be further explored in the future.

Informed Consent

The authors report no conflict of interest.

Availability of data and material

We declared that we embedded all data in the manuscript.

Authors' contributions

HT conducted the experiments and wrote the paper; LY conceived, designed the study and revised the manuscript.

Funding

None.

Acknowledgement

We thanked The Second Affiliated Hospital of Dalian Medical University approval our study.

References

- Ghafari-Fard S, Shoorei H, Taheri M (2020) Non-coding RNAs participate in the ischemia-reperfusion injury. *Biomed Pharmacother* 129:110419. doi: 10.1016/j.biopha.2020.110419
- Wu MY, Yiang GT, Liao WT, Tsai AP, Cheng YL, Cheng PW, et al (2018) Current mechanistic concepts in ischemia and reperfusion injury. *Cell Physiol Biochem* 46(4):1650-1667. doi: 10.1159/000489241
- Li M, Tang H, Li Z, Tang W (2022) Emerging treatment strategies for cerebral ischemia-reperfusion injury. *Neurosci* 507:112-124. doi: 10.1016/j.neuroscience.2022.10.020
- Zhang Q, Jia M, Wang Y, Wang Q, Wu J (2022) Cell death mechanisms in cerebral ischemia-reperfusion injury. *Neurochem Res*

- 47(12):3525–3542. doi: 10.1007/s11064-022-03697-8
5. Derex L, Cho TH (2017) Mechanical thrombectomy in acute ischemic stroke. *Revue neurologique* 173(3):106–113. doi: 10.1016/j.neurol.2016.06.008
 6. Krishnan R, Mays W, Elijevich L (2021) Complications of mechanical thrombectomy in acute ischemic stroke. *Neurology* 97(20 Suppl 2):S115–S125. doi: 10.1212/WNL.0000000000012803
 7. Correia de Sousa M, Gjorgjieva M, Dolicka D, Sobolewski C, Foti M (2019) Deciphering miRNAs' action through miRNA editing. *Int J Mol Sci* 20(24):6249. doi: 10.3390/ijms20246249
 8. Neag MA, Mitre AO, Burlacu CC, Inceu AI, Mihu C, Melincovici CS, et al (2022) miRNA involvement in cerebral ischemia-reperfusion injury. *Front Neurosci* 16:901360. doi: 10.3389/fnins.2022.901360
 9. Zhao H, Tao Z, Wang R, Liu P, Yan F, Li J, et al (2014) MicroRNA-23a-3p attenuates oxidative stress injury in a mouse model of focal cerebral ischemia-reperfusion. *Brain Res* 1592:65–72. doi: 10.1016/j.brainres.2014.09.055
 10. Deng B, Bai F, Zhou H, Zhou D, Ma Z, Xiong L, Wang Q (2016) Electroacupuncture enhances rehabilitation through miR-181b targeting PirB after ischemic stroke. *Sci Rep* 6:38997. doi: 10.1038/srep38997
 11. Yao X, Yao R, Yi J, Huang F (2019) Upregulation of miR-496 decreases cerebral ischemia/reperfusion injury by negatively regulating BCL2L14. *Neurosci Lett* 696:197–205. doi: 10.1016/j.neulet.2018.12.039
 12. Aguado-Fraile E, Ramos E, Sáenz-Morales D, Conde E, Blanco-Sánchez I, Stamatakis K, et al (2012) miR-127 protects proximal tubule cells against ischemia/reperfusion: identification of kinesin family member 3B as miR-127 target. *PLoS One* 7(9):e44305. doi: 10.1371/journal.pone.0044305
 13. Conde E, Giménez-Moyano S, Martín-Gómez L, Rodríguez M, Ramos ME, Aguado-Fraile E, et al (2017) HIF-1 α induction during reperfusion avoids maladaptive repair after renal ischemia/reperfusion involving miR127-3p. *Sci Rep* 7:41099. doi: 10.1038/srep41099
 14. Zhang Y, Tian C, Liu X, Zhang H (2020) Identification of genetic biomarkers for diagnosis of myocardial infarction compared with angina patients. *Cardiovasc Ther* 2020:8535314. doi: 10.1155/2020/8535314
 15. Fuernau G, Eitel I, Thiele H (2016) Smoke over myocardial infarction: cigarettes and reperfusion injury. *Eur Heart J* 37(36):2765–2767. doi: 10.1093/eurheartj/ehw111
 16. Rinker B, Fink BF, Stoker AR, Milan ME, Nelson PT (2013) Calcium channel blockers reduce the effects of cigarette smoking on peripheral nerve ischemia/reperfusion injury. *Ann Plast Surg* 70(2):222–226. doi: 10.1097/SAP.0b013e3182367be1
 17. Yang YY, Gong DJ, Zhang JJ, Liu XH, Wang L (2019) Diabetes aggravates renal ischemia-reperfusion injury by repressing mitochondrial function and PINK1/Parkin-mediated mitophagy. *Am J Physiol Renal Physiol* 317(4):F852–F864. doi: 10.1152/ajprenal.00181.2019
 18. Yang B, Li Y, Ma Y, Zhang X, Yang L, Shen X, et al (2021) Selenium attenuates ischemia/reperfusion injury-induced damage to the blood-brain barrier in hyperglycemia through PI3K/AKT/mTOR pathway-mediated autophagy inhibition. *Int J Mol Med* 48(3):178. doi: 10.3892/ijmm.2021.5011
 19. Lejay A, Fang F, John R, Van JA, Barr M, Thaveau F, et al (2016) Ischemia reperfusion injury, ischemic conditioning and diabetes mellitus. *J Mol Cell Cardiol* 91:11–22. doi: 10.1016/j.yjmcc.2015.12.020
 20. Pagliaro P, Penna C (2017) Hypertension, hypertrophy, and reperfusion injury. *J Cardiovasc Med (Hagerstown)* 18(3):131–135. doi: 10.2459/JCM.0000000000000435
 21. Du H, He Y, Zhu J, Zhou H, Shao C, Yang J, Wan H (2023) Danhong injection alleviates cerebral ischemia-reperfusion injury by inhibiting mitochondria-dependent apoptosis pathway and improving mitochondrial function in hyperlipidemia rats. *Biomed Pharmacother* 157:114075. doi: 10.1016/j.biopha.2022.114075
 22. Eltzschig HK, Eckle T (2011) Ischemia and reperfusion--from mechanism to translation. *Nat Med* 17(11):1391–1401. doi: 10.1038/nm.2507
 23. Christou CD, Tsoulfas G (2020) The role of microRNA in hepatic ischemia/reperfusion injury. *Microna* 9(4):248–254. doi: 10.2174/2211536609666200129162531
 24. Cannistrà M, Ruggiero M, Zullo A, Gallelli G, Serafini S, Maria M, et al (2016) Hepatic ischemia reperfusion injury: a systematic review of literature and the role of current drugs and biomarkers. *Int J Surg* 33(Suppl 1):S57–S70. doi: 10.1016/j.ijssu.2016.05.050
 25. Liang M, Yao W, Shi B, Zhu X, Cai R, Yu Z, et al (2021) Circular RNA hsa_circ_0110389 promotes gastric cancer progression through upregulating SORT1 via sponging miR-127-5p and miR-136-5p. *Cell Death Dis* 12(7):639. doi: 10.1038/s41419-021-03903-5
 26. Zhang J, Liu Z, Dong Y (2022) miR-127-5p Targets JAM3 to regulate ferroptosis, proliferation, and metastasis in malignant meningioma cells. *Dis Markers* 2022:6423237. doi: 10.1155/2022/6423237
 27. Zhang B, Li Q, Song Z, Ren L, Gu Y, Feng C, et al (2022) hsa_circ_0000285 facilitates thyroid cancer progression by regulating miR-127-5p/CDH2. *J Clin Lab Anal* 36(7):e24421. doi: 10.1002/jcla.24421
 28. Liang J, Xu L, Zhou F, Liu AM, Ge HX, Chen YY, Tu M (2018) MALAT1/miR-127-5p regulates osteopontin (OPN)-mediated proliferation of human chondrocytes through PI3K/Akt pathway. *J Cell Biochem* 119(1):431–439. doi: 10.1002/jcb.26200
 29. Liu C, Cheng P, Liang J, Zhao X, Du W (2021) Circular RNA circ_0128846 promotes the progression of osteoarthritis by regulating miR-127-5p/NAMPT axis. *J Orthop Surg Res* 16(1):307. doi: 10.1186/s13018-021-02428-z
 30. Liu H, Zhao H, Huang Y, Lei M (2023) Circ_0002715 promotes the development of osteoarthritis through regulating LXN by sponging miR-127-5p. *J Orthop Surg Res* 18(1):230. doi: 10.1186/s13018-023-03638-3
 31. Reich A, Spering C, Gertz K, Harms C, Gerhardt E, Kronenberg G, et al (2011) Fas/CD95 regulatory protein Faim2 is neuroprotective after transient brain ischemia. *J Neurosci* 31(1):225–233. doi: 10.1523/JNEUROSCI.2188-10.2011
 32. Komnig D, Gertz K, Habib P, Nolte KW, Meyer T, Brockmann MA, et al (2018) Faim2 contributes to neuroprotection by erythropoietin in transient brain ischemia. *J Neurochem* 145(3):258–270. doi: 10.1111/jnc.14296
 33. Komnig D, Schulz JB, Reich A, Falkenburger BH (2016) Mice lacking Faim2 show increased cell death in the MPTP mouse model of Parkinson disease. *J Neurochem* 139(5):848–857. doi: 10.1111/jnc.13847
 34. Habib P, Stamm AS, Zeyen T, Noristani R, Slowik A, Beyer C, et al (2019) EPO regulates neuroprotective Transmembrane BAX Inhibitor-1 Motif-containing (TMBIM) family members GRINA and FAIM2 after cerebral ischemia-reperfusion injury. *Exp Neurol* 320:112978. doi: 10.1016/j.expneurol.2019.112978